Preprints of the 19th World Congress
The International Federation of Automatic Control
Cape Town, South Africa. August 24-29, 2014

Simultaneous Actuation and Sensing for Electrostatic Drives in MEMS using Frequency Modulated Capacitive Sensing

Steven I. Moore * **S. O. Reza Moheimani** *

* *The University of Newcastle, Callaghan, NSW 2308 Australia*
(e-mail: steven.i.moore@uon.edu.au; Reza.Moheimani@newcastle.edu.au)

Abstract: This paper presents a displacement sensing technique that can be integrated into a microfabricated microelectromechanical system (MEMS) device. This sensor determines displacement by measuring the capacitance of a MEMS electrostatic drive, as the capacitance is a function of the displacement. The electrostatic drive is incorporated into an LC oscillator whose frequency varies with the capacitance. A lock-in amplifier is used to extract the frequency signal. The sensitivity of the sensor was $-1.153\,\mathrm{V}\,\mu\mathrm{m}^{-1}$ and exhibited no dynamics up to the 1.2 kHz bandwidth of the MEMS device it was implemented in. The electrostatic drive in this technique is used for both actuation and sensing. This effectively increases the transduction efficiency of both the actuator and sensor as more space on the die can be dedicated to the one drive. Additionally, the scheme allows for one terminal of the drive to be grounded. Thus, this scheme can be used on MEMS devices with more than one drive connected to a common mechanical structure which is electrically grounded.

1. INTRODUCTION

Microelectromechanical systems (MEMS) are microfabricated mechanical systems which benefit from batch production, miniaturization and precision fabrication associated with microfabrication (Liu, 2011). MEMS in general interact more strongly with the physical world than microfabricated electrical circuits, thus, they have found application in a broad range of sensors (Bryzek et al., 2006; Khoshnoud & de Silva, 2012b). Many of these devices require displacement measurements of the mechanical system to function. Other applications of displacement sensors include nanopositioning (Zhu, Bazaei, Moheimani, & Yuce, 2011), adaptive optics (Xu, Feng, Li, & Chu, 2008) and a variety of biomedical devices (Khoshnoud & de Silva, 2012a). Displacement measurements in these systems are characterized by ranges in order of nanometers to micrometers, and resolutions down to the order of nanometers.

A number of mechanisms have been used to measure displacement on the nanoscale (Fleming, 2013). Thermal sensors (Fowler, Bazaei, & Moheimani, 2013) have a small die footprint, low operating voltage and high resolution, but suffer from low bandwidth and high power consumption. Piezoresistive sensors (Barlian, Park, Mallon, Rastegar, & Pruitt, 2009) are simple to implement and have high resolution. They suffer from a low range, poor thermal and long-term stability and non-linearities. There are a number of optical measurement techniques including laser Doppler vibrometry (Castellini, Martarelli, & Tomasini, 2006) and interferometry (Fleming, 2013). These devices provide excellent resolution and range. However, they are of significant size and cost. Their incorporation into a MEMS device is, therefore, not viable. Capacitive sensors are investigated in this paper for displacement measurement. They are simple to implement in MEMS and consume no power. However, they require more complex readout circuitry and consume significant die space.

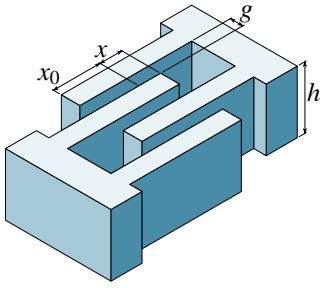

Figure 1. Shown is a rendering of part of a comb drive. One of the combs is fixed, while the other can move with one degree of freedom. The dimensions used in equation 1 are shown. The parameter n of equation 1, which is the number of overlapping faces, in this diagram is 3.

There are a number of topologies for electrostatic drives in MEMS. A very common topology is the comb drive (Kaajakari, 2009). A rendering of a comb drive is shown in figure 1. This electrostatic drive keeps the gap between the electrodes constant, while the overlap between the electrodes changes. Parameters of this drive are the electrode thickness h, the permittivity of the dielectric ε, the zero volt overlap x_0 and the electrode gap g. Comb drives consist of a number of parallel electrodes. The parameter n is defined as the number of overlapping faces in the comb drive. The relationship between drive's capacitance and displacement is:

$$C = \frac{n\varepsilon h\,(x_0 + x)}{g}. \tag{1}$$

Equation 1 shows that a measurement of capacitance can be used to derive a displacement signal. In a comb drive, the force generated is independent of displacement and the mapping between capacitance and displacement is linear.

The target application for the capacitive sensing outlined in this paper is nanopositioning. The nanopositioner it is applied

to is shown in figure 2 (Fowler, Laskovski, Hammond, & Moheimani, 2012). The design of the readout circuitry is influenced by two characteristics of this nanopositioner. Firstly, the silicon on insulator microfabrication processes cannot provide electrical isolation on the mechanical structure. To isolate the operation of the two drives, the mechanical structure is grounded. The readout circuitry must deal with the grounded electrostatic drives. Secondly, to increase the actuation and sensing transduction efficiency, the same drive is to be used by both functions. The readout circuitry must be able to isolate itself from the actuation signal. There are a number of methods to readout the capacitance (Huang, Stott, Green, & Beck, 1988).

A number of implementations of capacitive sensing in MEMS are already published. Chu and Gianchandani (2003) produced a positioner that electrically isolates the actuation and sensing systems. However, not all microfabrication processes allow this. Lee, Huang, and Chu (2009) use an AC bridge readout circuit. This requires the common node not be grounded. This scheme cannot be used with two capacitive drives. Zhu, Moheimani, and Yuce (2011) use the MS3110 IC which is an implementation of a charge/discharge method. This system requires electrically isolated capacitors. Carminati, Ferrari, Guagliardo, and Sampietro (2011) use an AC bridge circuit implemented with a transimpedance amplifier. This cannot be applied to systems with more than one capacitive drive attached to the common mechanical structure.

There are a number of simultaneous actuation and displacement sensing schemes published for MEMS electrostatic drives. Of advantage is being able to dedicate more capacitive infrastructure to a single drive, increasing the transduction efficiency of both systems. Nieminen, Hyyryläinen, Veijola, Ryhänen, and Ermolov (2005) measure the capacitance by measuring the reflection of a 836 MHz wave injected into the drive. One terminal of the drive is grounded. A low frequency actuation voltage and the high frequency sense voltage are combined on the other terminal. Dong and Ferreira (2008) measure the capacitance by injecting a high frequency voltage across the capacitor and measuring the current associated with it. An adder is used to combine the sensing and actuation signals. A shunt resistor is used to measure the current through the capacitor. The combination of the capacitor and shunt resistor are used to filter the low frequency actuation signal out from the sense signal. Liang, Xiaowei, Weiping, and Zhiping (2011) implement simultaneous actuation and sensing using a switching scheme to alternate the connection of the two systems to the electrostatic drive. This scheme is widespread in inertial sensors due to its suitability to be implemented in CMOS circuits. The capacitive sensor in this case uses switching to charge and discharge the capacitor with a constant voltage. The amount of charge flowing off the capacitor on the discharge is measured with a charge amp providing a signal proportional to capacitance.

This paper presents a simultaneous actuation and displacement sensing technique for a MEMS nanopositioner using electrostatic drives. An oscillator type capacitive sensing technique is used as an alternative to the typical AC bridge technique. This technique involves incorporating the drive into an LC oscillator. Oum, Lee, Kim, and Hong (2008) and Laskovski, Yuce, and Moheimani (2013) implement similar capacitive readout circuitry in other mechatronic systems. The proposed transducer is applied to grounded electrostatic drives. This allows it to be applied to systems with multiple drives electrically connected to a common mechanical structure.

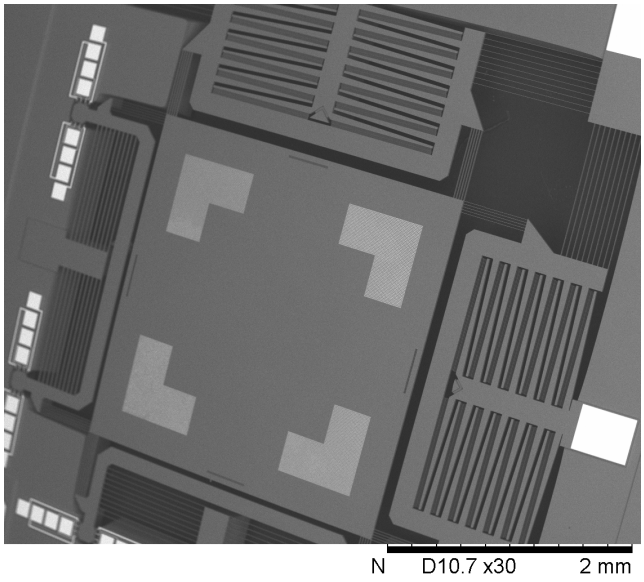

Figure 2. Shown is a SEM image of the nanopositioner that the simultaneous sensing and actuation technique is demonstrated on. To the top and right of the image are the comb drives used to displace the stage in the center.

Section 2 outlines the implementation of the simultaneous actuation and sensing transduction technique. This includes a quick overview of the nanopositioner it is demonstrated on and the circuitry used to implement the transduction technique. Section 3 presents the results of experiments to show the system functioning, the sensitivity of the sensing scheme and the dynamics over the bandwidth of the nanopositioner.

2. THE DESIGN

The nanopositioner upon which the transduction technique is applied is described by Fowler et al. (2012). A scanning electron microscope (SEM) image of the nanopositioner is shown in figure 2. The resonance frequency of each axis of the nanopositioner is 820 Hz. A displacement of 15 µm can be achieved with 45 V applied to a capacitive drive.

The simultaneous sensing and actuation technique operates by decoupling the actuation and sensing signals on a electrostatic drive by frequency. Given the bandwidth of the nanopositioner, the actuation signal need only contain frequencies up to 10 kHz. The frequency of the sensing signal was chosen at 50 MHz.

The schematic implementing the transduction technique is shown in figure 3. It shows an LC oscillator with the nanopositioner incorporated into its resonator. The displacement is determined by measuring the capacitance of the electrostatic drive on the nanopositioner. As the capacitance of the drive changes, the frequency of the oscillator will change. The frequency signal is converted to voltage to extract the displacement signal.

The low frequency actuation signal is combined with the high frequency LC oscillator signal on the nanopositioner's electrostatic drive. An inductor is used to suppress high frequency signals from traveling back into the actuation system. Capacitors are used to suppress feedthrough of the low frequency actuation signal into the sensing system.

In the following experiments, the electrostatic drives are biased at 25 V. The capacitance of the drives was measured with an

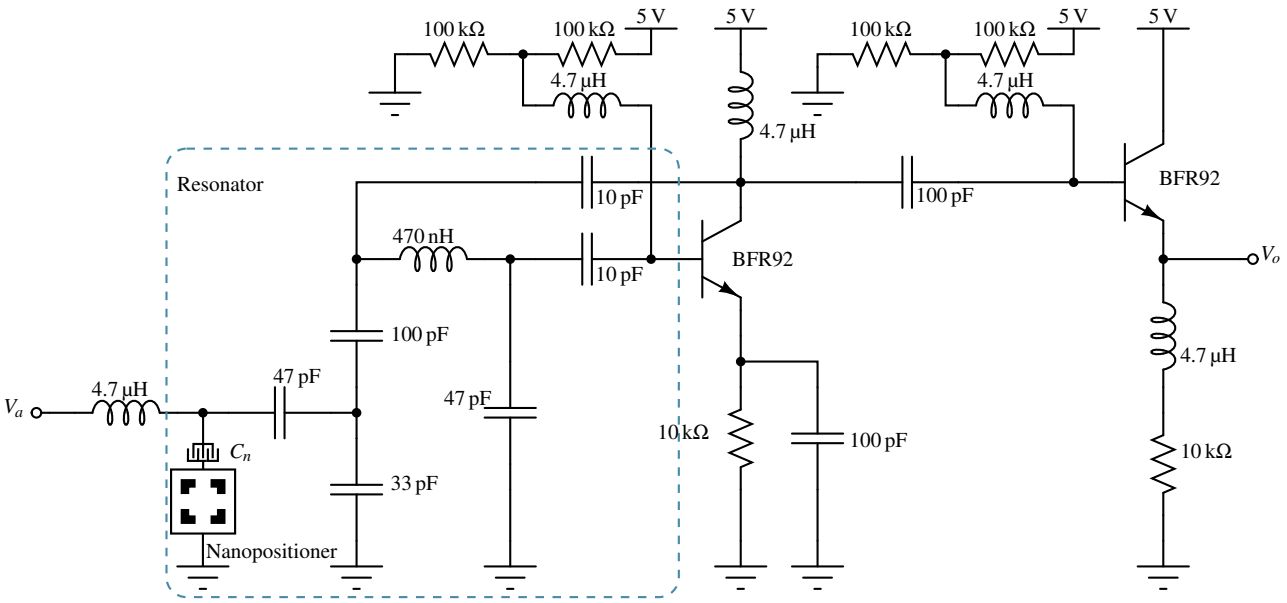

Figure 3. The schematic of the LC oscillator which converts displacement to frequency. From left to right the parts of the system are: the actuation input, the resonator, the sustaining amplifier and the output buffer. Capacitance C_n is the electrostatic drive of the nanopositioner and has been incorporated into the resonator.

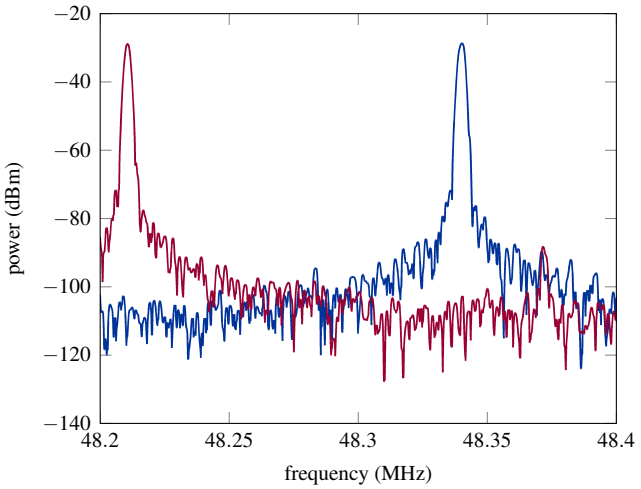

Figure 4. The oscillator spectrums at the extents of the frequency swing as the nanopositioner is actuated. The spectrums show the oscillator is producing a sinusoidal output. The frequency is oscillating between 48.211 MHz and 48.34 MHz with a 3 V_{pp} input voltage.

LCR meter. At this bias condition the drives have a capacitance of 8.79 pF. The frequency of the oscillator is found by analyzing the resonator highlighted in figure 3. The center frequency of the oscillator is 50.4 MHz.

3. RESULTS

The first experiment is to show the correct functioning of the oscillator as the drive is actuated. The input voltage is set to a 1 Hz 3 V_{pp} triangular wave. A gain of 5 is applied to this voltage then biased by 25 V before being applied to the electrostatic drive. The output of the oscillator is fed into a spectrum analyzer with an AC coupled 50 Ω input impedance. The spectrum analyzer showed a peak whose frequency oscillated back and forth with the 1 Hz input frequency. The frequency of the oscillator was

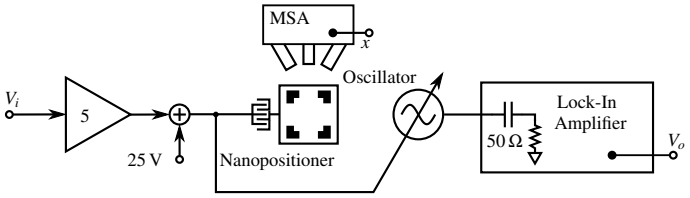

Figure 5. The schematic of the experimental setup. The input voltage is amplified by 5 and biased by 25 V before being applied to the nanopositioner's electrostatic drive. The output of the oscillator is fed into a lock-in amplifier which has a conversion gain of 100 µV Hz^{-1}. The displacement measurement is made with a micro system analyzer (MSA).

modulated from 48.211 MHz to 48.34 MHz. The spectrum of the signal at these two frequencies are shown in Figure 4.

Next the experimental setup in Figure 5 was used to determine sensitivity and dynamics of the sensor. Again the input signal is amplified by 5 and biased by 25 V. The output of the oscillator is fed into a lock-in amplifier for frequency demodulation. The lock-in amplifier has an AC coupled 50 Ω input impedance. For comparison, a displacement measurement is made using a micro system analyzer (MSA) consisting of laser Doppler vibrometers.

To test the low frequency characteristics of the system, the input V_i was set to a 1 Hz 3 V_{pp} triangular wave. The resulting displacement from the MSA and the oscillator frequency from the lock-in amplifier are plotted in Figure 6. The peak to peak displacement is 6.243 µm and the peak to peak frequency is 72 kHz. This gives a low frequency gain of 11.53 kHz µm^{-1}. The other characteristic of note is the 180° phase shift between the two signals. There is a differences in the carrier frequency and sensitivity between this experiment and the previous one shown in Figure 4. The differences indicate the presence of drift in the current sensor setup.

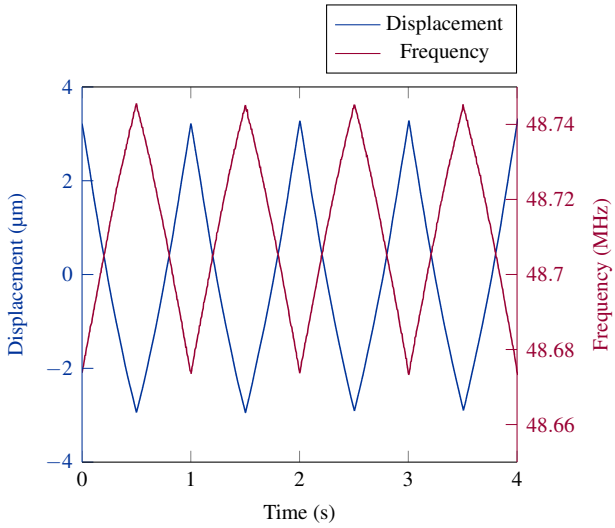

Figure 6. This plot shows the nanopositioner's displacement signal and the lock-in amplifier's frequency signal. These are measured while the input is set to a 1 Hz 3 V_{pp} triangular wave.

The frequency response from the input V_i to displacement x and from the input V_i to the lock-in amplifier output V_o are used to characterize the dynamics of the sensor. The measurements are performed in a frequency band that is of concern for the nanopositioner in use with this system. The frequency band is from 100 Hz to 1.2 kHz. The frequency response from the input to displacement is performed with the MSA. The frequency response from the input to the lock-in amplifier output is performed with a signal analyzer. The frequency from the lock-in amplifier was converted to a voltage signal at 100 µV Hz^{-1}. The responses are plotted in Figure 7. The frequency response shows no dynamics over the frequency band, only a gain and a phase shift of 180°.

4. CONCLUSION

This paper has demonstrated a simultaneous actuation and displacement sensing technique that can be used with MEMS electrostatic drives. The technique involves incorporating the electrostatic drive into an LC oscillator. As the capacitance of the drive changes with displacement, the frequency of the oscillator will change. The paper has demonstrated this technique is feasible. This provides benefit to MEMS designers, in that die space does not need to be split between actuation and sensing systems. This simplifies MEMS designs and increases the transduction efficiency of both systems. The results showed the sensitivity of the sensor was −1.153 V μm^{-1}. More importantly, no dynamics were observed in the sensor up to the 1.2 kHz bandwidth of the nanopositioner. This allows the technique to be used in feedback control of nanopositioners and other MEMS devices. Further refinement of the design is needed. To provide a fully integrated solution, the lock-in amplifier needs to be replaced by a FM detector circuit. Also, the design would likely benefit from a better oscillator design to minimize phase noise. With the refinements, the resolution of the sensor needs to be measured. This is the critical metric to evaluate the performance of the technique and compare it to other solutions.

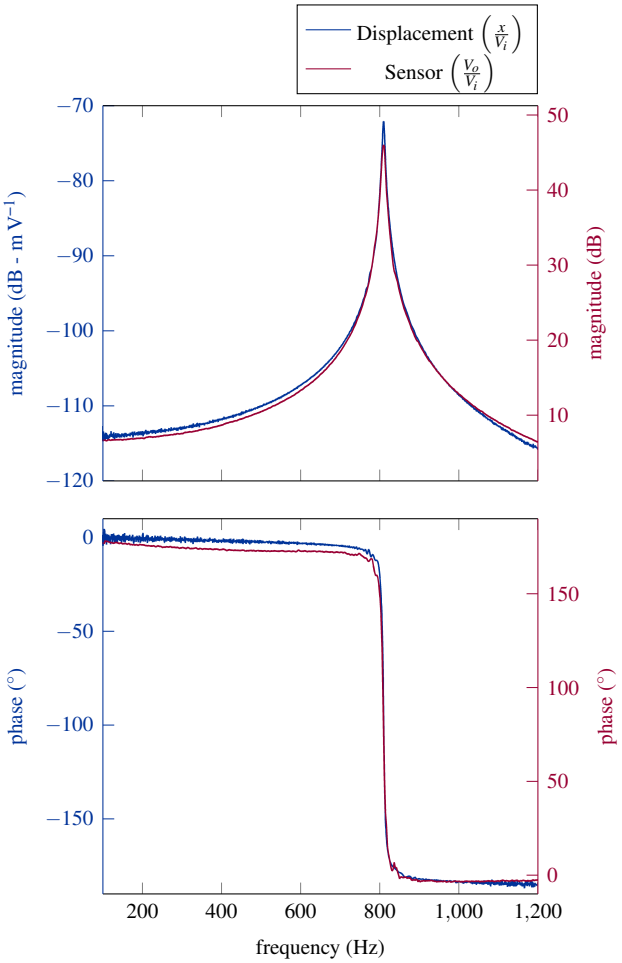

Figure 7. The frequency response of the nanopositioner. Both frequency responses are with respect to the input voltage. The substantial difference between the two responses is a 121 dB gain and a 180° phase shift.

REFERENCES

Barlian, A., Park, W.-T., Mallon, J., Rastegar, A., & Pruitt, B. (2009). Review: semiconductor piezoresistance for microsystems. *Proceedings of the IEEE*, *97*(3), 513–552.

Bryzek, J., Roundy, S., Bircumshaw, B., Chung, C., Castellino, K., Stetter, J., & Vestel, M. (2006). Marvelous MEMS. *Circuits and Devices Magazine, IEEE*, *22*(2), 8–28.

Carminati, M., Ferrari, G., Guagliardo, F., & Sampietro, M. (2011). Zeptofarad capacitance detection with a miniaturized CMOS current front-end for nanoscale sensors. *Sensors and Actuators A: Physical*, *172*(1), 117–123.

Castellini, P., Martarelli, M., & Tomasini, E. (2006). Laser doppler vibrometry: development of advanced solutions answering to technology's needs. *Mechanical Systems and Signal Processing*, *20*(6), 1265–1285.

Chu, L. L. & Gianchandani, Y. B. (2003). A micromachined 2D positioner with electrothermal actuation and sub-nanometer capacitive sensing. *Journal of Micromechanics and Microengineering*, *13*(2), 279.

Dong, J. & Ferreira, P. M. (2008). Simultaneous actuation and displacement sensing for electrostatic drives. *Journal of Micromechanics and Microengineering*, *18*(3), 035011.

Fleming, A. J. (2013). A review of nanometer resolution position sensors: operation and performance. *Sensors and Actuators A: Physical*, *190*, 106–126.

Fowler, A. G., Bazaei, A., & Moheimani, S. O. R. (2013). Design and analysis of nonuniformly shaped heaters for improved MEMS-based electrothermal displacement sensing. *Microelectromechanical Systems, Journal of*, *22*(3), 687–694.

Fowler, A. G., Laskovski, A. N., Hammond, A. C., & Moheimani, S. O. R. (2012). A 2-DoF electrostatically actuated MEMS nanopositioner for on-chip AFM. *IEEE/ASME Journal of Microelectromechanical Systems*, *21*(4), 771–773.

Huang, S. M., Stott, A. L., Green, R. G., & Beck, M. S. (1988). Electronic transducers for industrial measurement of low value capacitances. *Journal of Physics E: Scientific Instruments*, *21*(3), 242.

Kaajakari, V. (2009). *Practical MEMS*. Small Gear Publishing.

Khoshnoud, F. & de Silva, C. (2012a). Recent advances in MEMS sensor technology - biomedical applications. *Instrumentation Measurement Magazine, IEEE*, *15*(1), 8–14.

Khoshnoud, F. & de Silva, C. (2012b). Recent advances in MEMS sensor technology – mechanical applications. *Instrumentation Measurement Magazine, IEEE*, *15*(2), 14–24.

Laskovski, A. N., Yuce, M., & Moheimani, S. O. R. (2013, September). Fm-based piezoelectric strain voltage sensor at ultra-low frequencies with wireless capability. *Sensors & Actuators: A. Physical*, *199*, 49–55.

Lee, J.-I., Huang, X., & Chu, P. (2009). Nanoprecision mems capacitive sensor for linear and rotational positioning. *Microelectromechanical Systems, Journal of*, *18*(3), 660–670.

Liang, Y., Xiaowei, L., Weiping, C., & Zhiping, Z. (2011). High resolution interface circuit for closed-loop accelerometer. *Journal of Semiconductors*, *32*(4), 045005.

Liu, C. (2011). *Foundations of MEMS*. Prentice Hall.

Nieminen, H., Hyyryläinen, J., Veijola, T., Ryhänen, T., & Ermolov, V. (2005). Transient capacitance measurement of MEM capacitor. *Sensors and Actuators A: Physical*, *117*(2), 267–272.

Oum, J., Lee, S. E., Kim, D.-W., & Hong, S. (2008). Noncontact heartbeat and respiration detector using capacitive sensor with colpitts oscillator. *Electronics Letters*, *44*(2), 87–88.

Xu, X.-H., Feng, Y., Li, B.-Q., & Chu, J.-R. (2008). Integration of displacement sensor into bulk PZT thick film actuator for MEMS deformable mirror. *Sensors and Actuators A: Physical*, *147*(1), 242–247.

Zhu, Y., Bazaei, A., Moheimani, S. O. R., & Yuce, M. R. (2011, June). Design, modeling, and control of a micromachined nanopositioner with integrated electrothermal actuation and sensing. *Microelectromechanical Systems, Journal of*, *20*(3), 711–719.

Zhu, Y., Moheimani, S. O. R., & Yuce, M. R. (2011). Simultaneous capacitive and electrothermal position sensing in a micromachined nanopositioner. *Electron Device Letters, IEEE*, *32*(8), 1146–1148.